Environmental Science
Processes & Impacts

Diversity of Organic Components in Airborne Waste Discharged from Sewer Pipe Repairs

Journal:	*Environmental Science: Processes & Impacts*
Manuscript ID	EM-ART-02-2023-000084.R2
Article Type:	Paper

Diversity of Organic Components in Airborne Waste Discharged from Sewer Pipe Repairs

Ana C. Morales,[1] Christopher P. West,[1] Brianna N. Peterson,[1] Yoorae Noh,[2] Andrew J. Whelton,[2,3] Alexander Laskin[1,*]

[1]College of Science, Department of Chemistry, [2]Lyles School of Civil Engineering, [3]Division of Environmental and Ecological Engineering, Purdue University, West Lafayette, IN, USA

Submission prepared for:
Environmental Science: Processes and Impacts

August 30, 2023

Abstract

Air-discharged waste from commonly used trenchless technologies of sewer pipe repairs is an emerging and poorly characterized source of urban pollution. This study reports on the molecular-level characterization of the atmospherically discharged aqueous-phase waste condensate samples collected at four field sites of the sewer pipe repairs. The molecular composition of organic species in these samples was investigated using reversed-phase liquid chromatography coupled with a photodiode array detector and a high-resolution mass spectrometer equipped with interchangeable atmospheric pressure photoionization and electrospray ionization sources. The waste condensate components comprise a complex mixture of organic species that can partition between gas-, aqueous-, and solid-phases when water evaporates from the air-discharged waste. Identified organic species have broad variability in molecular weight, molecular structures, and carbon oxidation state, which also varied between the waste samples. All condensates contained complex mixtures of oxidized organics, N- and S-containing organics, condensed aromatics, and their functionalized derivatives that are directly released to the atmospheric environment during installations. Furthermore, semi-volatile, low volatility, and extremely low volatility organic compounds comprise 75 – 85% of the total compounds identified in the waste condensates. Estimates of the component-specific viscosities suggest that upon evaporation of water waste material would form the semi-solid and solid phases. The low volatilities and high viscosities of chemical components in these waste condensates will contribute to the formation of atmospheric secondary organic aerosols and atmospheric solid nanoplastic particles. Lastly, selected components expected in the condensates were quantified and found to be present at high concentrations (1 – 20 mg L^{-1}) that may exceed regulatory limits.

Environmental Significance Statement

Repair of sewer pipes in urban areas using trenchless cured-in-place-pipe technology emits a complex mixture of organic species partitioning between the gas-, aqueous-, and solid-phases. Here we report detection of substantial amounts of semi-, low-, and extremely low-volatility organic compounds in the air-discharged waste condensate that contribute to the production of organic aerosol and environmental nanoplastics.

Introduction

Cured-in-place-pipes (CIPP) are common, cost-efficient, trenchless technologies used to repair sanitary sewer, storm sewer, and drinking water pipes.[1] The CIPPs are created by inserting and inflating a flexible resin tube inside the damaged pipe, and then curing that resin tube into a hard plastic. Polymerization reactions in the resin are initiated by using heat or by ultraviolet light.[2] The most popular and least expensive curing approach involves blowing steam through the uncured resin tube and out an exhaust pipe into the air.[3] Until 2017, emissions from this operation were reported to only contain a small amount of gas-phase volatile organic compound (VOC) styrene near 3 ppm_v.[4] Follow-up work by others however indicated levels greater than 1,000 ppm_v styrene were also present.[5,6] Additional work found styrene levels were diluted in the ambient air, as suggested by dispersion model analysis.[2,7] However, field measurements showed that very complex and highly dynamic mixtures of multi-component chemical pollutants are in fact emitted into the atmospheric environment around the installation sites.[4,8,9] Although the chronic effects from occupational exposure require additional scrutiny,[10] acute environmental impacts of the chemicals and particulates in the emission plume have been associated with air pollution and human toxicity.[4,11,12] In some reports,[4] it has been noted that staff working in close proximity to the chemical emission plume lacked knowledge-based requirements for personal protection.[13–15] These installations have led to more than 146 reports of ambient and indoor air contamination incidents that affected schools, daycare centers, homes, offices, and even prompted building evacuations.[4,5,16–18] However, the composition of these emissions remains ambiguous.[19]

In order to understand the complex, multiphase emissions, it is important to systematically investigate all aspects of the installation process, including the chemical composition of different resin types. Styrene-based vinyl resins (S-based) are commonly employed for CIPP manufacture. The U.S. Environmental Protection Agency lists gas-phase styrene as a controlled hazardous air pollutant because of its toxicological concerns as a carcinogenic and endocrine disrupting compound.[4,19] Material safety data sheets (SDS) report 30–50 wt.% of the resin is composed of the monomer styrene.[20] However, the remaining resin constituents and their subsequent concentrations are not commonly reported by manufacturers.[19,21,22] Recent efforts have investigated the chemical composition of different resin types employed for pipe repair.[17,19,23] When investigating the composition of an S-based resin, Noh et al. (2022) found that the uncured resin contained 39 wt.% of VOCs, including the endocrine disrupting compounds styrene, 2-

ethylhexanoic acid, 1,3,5-trimethylbenzene, and hydroquinone.[19] To reduce volatile emissions, non-styrene resins, referred to as low-VOC vinyl ester-based (VE-based), are also employed.[19] For one VE-based resin type, the SDS described the resin as being a "styrene and monomer-free resin" with "no hazardous air pollutants or VOCs", however it was found that a low amount of styrene was in fact present in the VE-based resin.[19,24] Furthermore, the same study revealed that VE-based resins contain additional hazardous air pollutants (e.g., toluene and xylene), acrylate monomers (e.g., methacrylic acid and ethylene glycol dimethacrylate), and plasticizers (e.g., dibutyl maleate) that were absent in the S-based resin.[19]

Many studies have quantified the amount of gas-phase styrene released due to its high abundance in the S-based resins.[4,8,25–28] In 2015, a Los Angeles, California study revealed styrene exited three sewer pipe manholes during steam curing at a range of 250 – 1070 ppm_v.[6] In 2019, industry-backed researchers reported concentration of 1,820 ppm_v styrene in air at one worksite and multiple occurrences of >100 ppm_v styrene at other sites.[29] It should be noted that the USEPA regulatory limit for 8 hours of exposure to styrene in air is 0.085 ppm_v,[30] thus the styrene concentrations at the points of emission by these installations have exceeded the regulatory limit up to ~50,000 times. Previous investigations have also showed that more than 60 other VOCs were also released from raw S-based resins during storage and more than 20 additional VOCs were further released onsite during the installation procedure.[5] VOC levels have been reported up to ~6,200 ppm_v,[4] which is factor of $>10^5$ higher than background VOC concentrations (<100 ppb_v) reported even for heavily polluted urban areas.[31]

Previous reports identified formation of solid nanoplastic particles from drying droplets of the discharged waste and larger microplastic particles originated from mechanical removal of small fragments of cured composites and uncured resin.[4,9] Mixtures of styrene and non-styrene components of the discharged waste have recently been suggested to undergo unintended oligomerization reactions accelerated in the evaporating waste droplets, leading to the formation of highly viscous organic aerosols (OA) termed environmental nanoplastic (EnvNP) particles.[9] Moreover, it has been found that multiple monomer gas-phase compounds, resin constituents, and degradation products from incomplete curing reactions are present in emissions, all of which can react in the emission plume to produce unintended EnvNP byproducts.[8,12,19] However, it is currently unclear what specific species govern formation of these particles. The composition and physical properties of the air-discharged fragments of composite and partially cured resin materials

are highly variable because the uneven extent of polymerization, side reactions, and various effects of environmental aging.[17,19] It is essential to understand the sources and formation of OA as they have implications for air quality, human health, and the environment. Therefore, it is necessary to comprehensively investigate the molecular composition of waste emissions from CIPP operated with different resin materials to gain insights into composition and formation mechanisms of the air discharged EnvNP.

In this work, we investigate the chemical composition of four discharged waste condensates collected at selected field installation sites. We employ the advanced multi-modal analytical technique of high-performance liquid chromatography separation interfaced with a photodiode array detector and high-resolution mass spectrometer (HPLC-PDA-HRMS) for untargeted screening of the organic components in complex waste mixtures. Numerous species were detected and characterized in each sample, spanning a wide range of molecular weights, elemental formulas, and structures. Estimates of the volatility and viscosity values of individual components based on empirical models[32–34] suggest that most of the detected species will partition into condensed-phase particles, promoting formation and growth of OA and EnvNP at the installation sites. We also quantified select individual components in each of the four waste condensates to facilitate comparison of our study with previous reports. Overall, our results suggest an additional considerable source of urban air pollution from broadly used sewer pipe repairs, which require systematic evaluation.

Experimental Methods

Sample Collection. Samples of the discharged waste steamed into the air from sewer pipe installations were collected using ice-containing cold traps at outdoor locations in Sacramento, California in August 2016.[4] Detailed descriptions of the field sites (X1, X2, X4, X5) and the methods of sample collection have been reported elsewhere.[4] Briefly, at each site, stainless steel air manifolds were installed to cold-trap atmospherically discharged waste emitted at the steam CIPP exhaust point. The discharged steam-laden waste was sampled at ambient conditions, using ice chest condensers, and collected in Pyrex® bottles.[4] After collection, samples were stored at –20 °C pending analysis, which was performed in December 2019. Hereafter, the samples are referred to as waste condensates. Multiple samples were collected during each CIPP manufacture and the results of several of those samples are presented in this manuscript.

Two types of resins were used at the installation sites: an S-based resin and a VE-based non-styrene resin. At sites X1, X4, and X5 (X1-4-5 hereafter), the S-based resin was used (Vipel® L713-LTA-12 isophthalic based polyester resin; contains 32.0% of styrene monomer by weight; 0.5% Trigonox® KSM and 1% di-(4-tert-butylcyclohexyl) peroxy dicarbonate initiators). At site X2, the VE-based resin was used (EcoTek™ L040-TNVG-33 vinyl ester resin; contains 30 – 35 wt.% tripropylene glycol diacrylate monomer by weight; initiators were not disclosed). Table I summarizes four waste condensates used in this study and the corresponding concentrations of total organic carbon (TOC), dissolved organic carbon (DOC), styrene and seven other quantified species. Styrene concentration in condensates was characterized by GC-MS-TQ8040 (Shimadzu Co.). Quantification of samples was performed using 1 ppm of 1,4-dichlorobenzene-d4 (Supelco, Inc.) as an internal standard. Due to limited sample volume, the styrene concentration was not quantified for samples X2 or X5. The total organic carbon (TOC) concentration was measured using a TNM-L ROHS (Shimadzu Co.) analyzer in accordance with USEPA method 415.1.[35] In order to measure the dissolved organic carbon level, the samples were filtrated by a 0.5 μm glass fiber filter (Fisher Scientific) and measured with the same method for TOC. Values of selected standardized risk-based screening levels (SL) recommended by the Environmental Protection Agency (EPA) of USA for ground water protection[36] are included for comparison. Reported concentrations are in the units of milligrams of organic material per liter (mg L^{-1} or ppm) of the collected discharged waste condensate.

Table 1. Summary of waste condensates used in this study and the corresponding concentrations of their bulk and selected individual organic components.[9] Reported concentrations are in the units of milligram of organic material per liter (mg/L = ppm) of the collected discharged aqueous condensate.

		Waste Condensate Samples					EPA recommended Screening Levels (SL)	
		X1	**X2**	**X4**	**X5**			
ID Number	Styrene resin (Y/N)	Yes	No	Yes	Yes	logK_{ow}	Carcinogenic SL[a]	Noncarcinogenic SL[b]
	Total organic carbon	33.58 ± 0.83	133.40 ± 0.43	53.76 ± 0.46	13.18 ± 0.13	-	-	-
	Dissolved organic carbon	30.96 ± 0.55	127.20 ± 0.14	50.47 ± 0.36	12.71 ± 0.09	-	-	-
	Styrene	$(2.73 \pm 0.01)\times10^{0}$	-	$(1.07 \pm 0.18)\times10^{2}$	-	2.95	-	4.00×10^{0}
1	Benzoic acid	$(1.04 \pm 0.08)\times10^{1}$	$(8.74 \pm 0.67)\times10^{0}$	$(2.52 \pm 0.19)\times10^{0}$	$(2.22 \pm 0.17)\times10^{-1}$	1.87	-	8.00×10^{1}
2	Methyl methacrylate	$(1.76 \pm 0.25)\times10^{1}$	$(1.81 \pm 0.25)\times10^{1}$	$(2.50 \pm 0.35)\times10^{0}$	$(2.53 \pm 0.35)\times10^{0}$	1.38	-	2.80×10^{1}
3	Benzaldehyde	$(2.49 \pm 0.11)\times10^{0}$	$(2.44 \pm 0.11)\times10^{0}$	$(9.06 \pm 0.41)\times10^{-1}$	$(7.12 \pm 0.32)\times10^{-1}$	1.48	1.90×10^{-2}	2.00×10^{0}
4	Acetophenone	$(5.32 \pm 0.19)\times10^{-1}$	$(4.38 \pm 0.16)\times10^{-1}$	$(1.54 \pm 0.06)\times10^{-1}$	$(2.14 \pm 0.08)\times10^{-1}$	1.58	-	2.00×10^{0}
5	Tripropylene glycol diacrylate	$(1.99 \pm 0.04)\times10^{-2}$	$(1.95 \pm 0.42)\times10^{1}$	$(1.81 \pm 0.04)\times10^{-2}$	$(6.17 \pm 0.13)\times10^{-3}$	-	-	-
6	Dibutyl phthalate	$(3.42 \pm 0.01)\times10^{-2}$	$(1.41 \pm 0.10)\times10^{-2}$	$(2.11 \pm 0.09)\times10^{-2}$	$(1.33 \pm 0.06)\times10^{-2}$	4.5	-	2.00×10^{0}
7	Butylated hydroxytoluene	$(1.61 \pm 0.08)\times10^{-2}$	$(4.48 \pm 0.23)\times10^{-3}$	-	-	5.1	3.40×10^{-3}	6.00×10^{0}

[a] based on Target Risk of 10^{-6}

[b] based on CHILD Hazardous Index =1

Chemical Characterization. Solvent extracts of the waste samples were prepared using a 1:1 volumetric ratio of the original sample and a mixture of organic solvents with different polarity (acetonitrile/dichloromethane/hexane = 2/2/1 by volume). All solvents were Optima LC/MS grade, purchased from Fisher Chemical. This organic mixture was selected based on our previous studies[37,38] indicating that this mixture of solvents with different polarities yields the higher extraction efficiency for complex multi-component environmental mixtures, compared to extraction by pure water single component organic solvents.. The 1:1 *v:v* extraction mixtures were vortexed for 90 seconds to facilitate dissolution of organic materials in the solvent. The extracts were then filtered using syringe filters with 0.20 μm PTFE membrane to remove insoluble colloids. Filtered extracts were dried down to 100 μL remaining volume using a Turbo Vap nitrogen blowdown vortex evaporation system (Biotage) and reconstituted in 100 μL of acetonitrile. Visible precipitates formed during the preconcentration step, so all samples were filtered again using the PTFE syringe filters. A method blank of Optima LC/MS grade water was prepared following the discussed protocol.

The obtained extracts and method blank were analyzed using a high-performance liquid chromatography (HPLC) system (Vanquish) coupled with a photodiode array (PDA) detector and a high-resolution mass spectrometer (HRMS) Q Exactive HF-X (all components from Thermo Scientific, Inc). The chromatographic separation was performed using a reversed-phase column (Luna C18(2), 150 × 2 mm, 5 μm particles, 100 Å pores; Phenomenex, Inc.) following a revised version of elution protocol described in our previous studies.[37,39] A binary mobile phase was used consisting of: (A) water with 0.1% *v:v* formic acid and (B) acetonitrile with 0.1% *v:v* formic acid. A stepwise gradient of A+B mixture was employed at a flow rate of 200 μL/min: 0–3 min at 90% of A, 3–84 min a linear gradient from 90% to 0% of A, 84–100 min held at 0% of A, 100–101 min a linear gradient to 90% of A, and 101–120 min held at 90% of A to re-equilibrate the column at the initial mobile phase condition. The column was held at 25 °C and an injection volume of 20 μL was used for all samples. The PDA detector is equipped with a 1.0 cm fused silica LightPipe flow cell and a deuterium lamp light source. The absorbance was recorded in a wavelength range of 200 – 680 nm at a scan rate of 20 Hz and λ ± 2 nm spectral resolution. A solvent blank of 1:1 *v:v* acetonitrile/water was used to remove absorbance contributed by the solvent matrix. Absorbance values at wavelengths above 230 nm were considered for the samples to eliminate the background solvent absorption contribution.

Ionization of the HPLC-eluted analyte was performed using interchangeable electrospray ionization (ESI) and dopant-assisted atmospheric pressure photoionization (APPI) sources operating in positive and negative modes, covering a broad range of the analyte components with different polarities.[37,39,40] An Ion Max ion source (Thermo Scientific Inc.) was configured for either ESI(±) or APPI(±) operation. A mixture of 3-trifluoromethylanisole (TFMA; 98% purity, Alfa-Aesar) and chlorobenzene (1:99, v/v; anhydrous, 99.8% purity, Sigma-Aldrich) was used as the dopant to promote charge exchange and proton transfer reactions in the APPI mode.[37,41,42] Before entering the ionization source, the dopant was delivered to the HPLC outflow stream at a flow rate of 20 μL min^{-1} (10% of LC flow rate) using a syringe pump (Thermos, Inc.). It was found that the formic acid in the HPLC mobile phase caused substantial ion suppression in the APPI(–) mode,[37] therefore only APPI(+) and ESI(±) data sets were utilized in this study. HRMS data acquisition was performed at a mass range of m/z 80–1200 with a resolution of 240,000 at 200 m/z and at a scan rate of 1.5 Hz in full scan mode at an RF level of 80. Mass calibration was performed using commercial calibration solutions (Thermo Scientific, PI-88323 and PI-88324) ionized in ESI(±) modes.

Data Processing and Analysis. The HPLC-PDA -HRMS datasets were acquired using Xcalibur software (Thermo Inc.) and processed using the open-source software toolbox MZmine 2 (v. 2.51, http://mzmine.github.io/) to assist mass detection and extracted ion chromatogram construction. The ADAP chromatogram builder[43,44] was used for reconstruction of the extracted ion chromatograms followed by obtaining the output feature list using the following settings: a signal-to-noise threshold greater than 10:1, a minimum peak height of 10^4, HPLC peak duration range within 0.01-0.6 min, 10 min group size in the number of scans, and mass tolerance of 0.001 m/z. All raw Xcalibur data files were background-subtracted prior to data processing to remove the MS signals attributed to the solvent blank. The output feature list was visually inspected to remove non-retained chromatographic signals. The feature list containing the *m/z*, peak intensity, and retention times were exported into custom Excel macros that removed C^{13} isotopes followed by the grouping of homologous species based on the first order (CH_2) and the second order (CH_2, H_2) Kendrick mass defects.[45] Formular assignments of the group-representative species were performed using the MIDAS molecular formula calculator (v 1.1; National High Magnetic Field Laboratory, USA). For the extracted ions in the range of 80-1200 m/z, $[M+H]^+$, $[M+Na]^+$, and [M-

H]$^-$ were assumed to identify products in ESI(±) modes, while [M+H]$^+$and [M]$^{+\bullet}$ were assumed for APPI(+) mode. The following molecular constraints were applied for all formula assignments: $C_{1\text{-}70}$, $H_{1\text{-}100}$, $N_{0\text{-}5}$, $O_{0\text{-}50}$, $S_{0\text{-}1}$, and $Na_{0\text{-}1}$ for ESI(+) only. Assignments were limited to a mass tolerance of ± 2 ppm. Unassigned peaks are likely a result of either additional elements or multiply charged ions which are not considered by the assignment constraints. Additional assignment verifications were performed using customized in-house MATLAB script to correct for erroneous formula assignments based on elemental ratio limits discussed in previous reports.[46–49] Assigned formulas were then grouped into CHO, CHON, CHOS, and CHONS classes, based on their elemental composition.

The double bond equivalent (DBE)[50] values and aromaticity index (AI)[51,52] for the neutral species associated with the assigned ions were calculated using the following equations:

$$\mathrm{DBE} = C - H/2 + N/2 + 1 \quad (1)$$

$$\mathrm{AI} = \frac{1 + C - O - S - \frac{H}{2}}{C - O - N - S} \quad (2)$$

Saturation concentrations,[34] viscosity,[32] and nominal carbon oxidation states[53,54] of the identified species were calculated using equations summarized in Supplementary Note 1 of the SI file.

Results and Discussion

Figure 1 illustrates representative HPLC-PDA chromatograms recorded for four analyzed waste condensates. In all cases, complex mixtures of many strongly absorbing chromophores are observed throughout the entire elution time. Plausible species suggested for selected PDA features are listed in Table S1 (Supplementary Note 2). Several of these chromophores correspond to components of resin materials previously identified in the gas-phase emissions.[19] Specifically, benzoic acid ($C_7H_6O_2$), benzaldehyde ($C_7H_6O_2$), and acetophenone (C_8H_8O) are oxidized derivatives of styrene and possible decomposition products of the peroxide initiators[19] that strongly absorb UV light and they were identified in all four condensates. Additional chromophore species commonly identified in these four samples correspond to a few polycyclic aromatic hydrocarbons (PAHs), such as plausibly pyrene ($C_{16}H_{10}$) and benzo[*ghi*]perylene ($C_{22}H_{12}$), as inferred from

correlative assessment of HPLC-PDA and HPLC-APPI-HRMS chromatograms. Oxidized aromatics, such as the $C_{12}H_{10}O_2$, $C_{15}H_{12}O_2$, and $C_{16}H_{14}O$ species were also detected. The HPLC-PDA chromatograms in Figure 1 indicate both partial similarity and substantial variability in the range and abundance of chemical components present in waste condensates collected at different installation sites. In this study, we selected seven components labeled by dashed lines in Figure 1 for quantification. The complexity of each sample warrants future studies quantitatively investigating the gas and particle phase components.

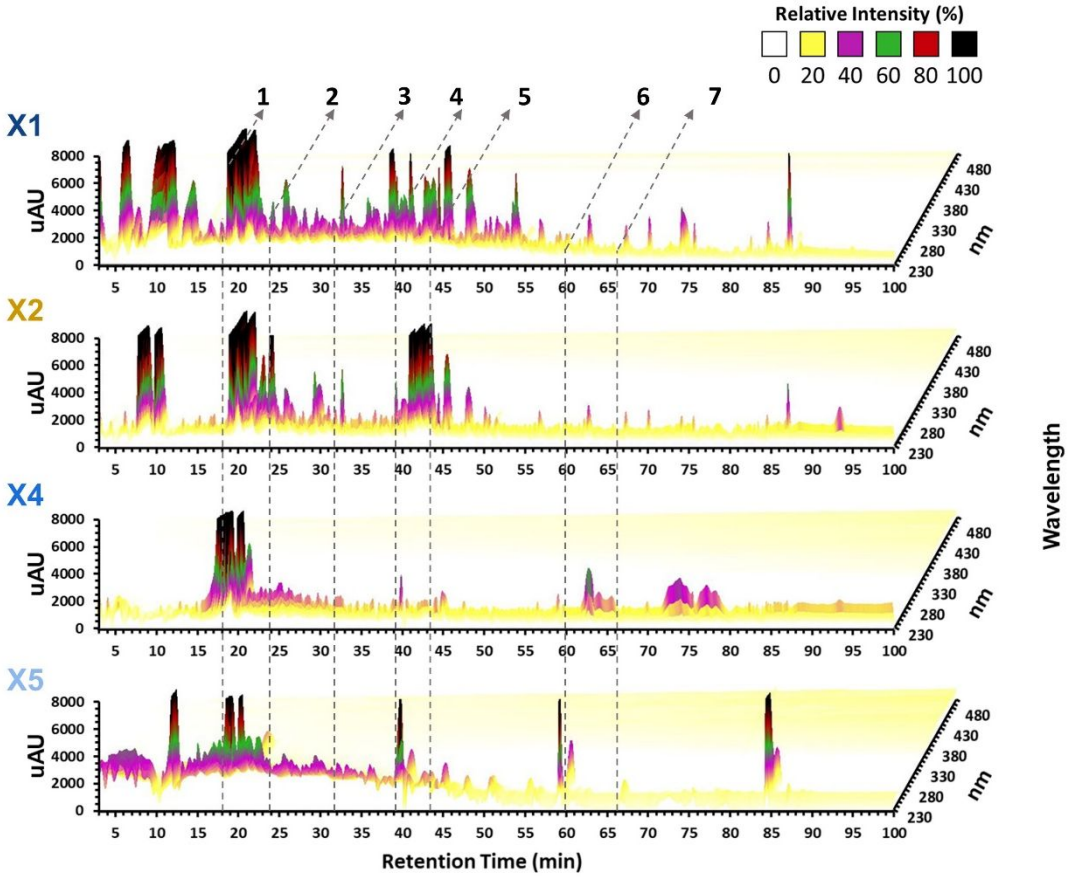

Figure 1. HPLC-PDA chromatograms of the solvent-soluble species extracted from each of four discharged waste condensates. The x-axis is retention time, the y-axis is the UV–vis absorbance (micro absorbance units, μAU), and the z-axis is the wavelength (nm). Dashed lines represent the seven selected compounds quantified in this study and are labeled based on their ID number in Table 1.

Figure 2 shows spectra of all ESI(±)-HRMS features detected in four waste condensates, while additional APPI(+)-HRMS spectra are included in Figure S1. All elemental assignments of organic species identified in the waste condensates based on the HRMS datasets are summarized

in the SI files (see Supplementary Note 3). The condensates exhibit very complex mixtures of different species that span a wide range of molecular weights, 80-800 g/mol (Figures 2 and S1). Numbers of assigned species ranged ~1800-2600 for ESI(+), ~600-1400 for ESI(−), and 37-139 for APPI(+), respectively. The assigned species accounted for a majority (62%-99%) of all detected ions in each mode. The wide range in total number of assigned species suggests high variations in molecular composition of the waste condensates. Of note, waste condensate from the X2 site, where the VE-based resin was used, shows a remarkably high number of assigned species, i.e., 2611 in ESI(+), 1415 in ESI(−), and 37 in APPI(+). This suggests that although the VE-based resin reduces the number of volatile components emitted to the gas phase, the condensed phase waste may have increased variability and concentrations of larger number of components than the S-based resin. Of three waste condensates from the sites where S-based resins were used (X1, 4-5), X1 contained the larger number of assigned species, i.e., 1813 in ESI(+), 596 in ESI(−), and 139 in APPI(+). It is expected that the waste condensates from the sites where S-based resins were used would have greater content of S-derived species susceptible for APPI(+) detection, which selectively ionizes aromatic compounds with lower oxygen content.[41,55–57] Higher fractions of aromatic species are apparent when comparing the total number of the APPI(+) detected species (48-139) in the waste condensate samples from X1-4-5 sites where S-based resins were employed, versus only 37 species found in the X2 condensate collected at the site with VE-based resin operation (Supplementary Note 4). Overall, all four waste condensates contain a large number of plausibly identified species that exhibit a much broader range than the lists of the gas-phase emission species investigated and reported in previous studies using GC-MS.[4,8,17,19,58] It follows that the condensed-phase waste emissions contain very complex mixtures of chemicals at each of the installation sites. Furthermore, these mixtures of organic species present in the steam laden waste emitted into the air will undergo aqueous-phase ageing chemistry leading to formation of OA.[59–62]

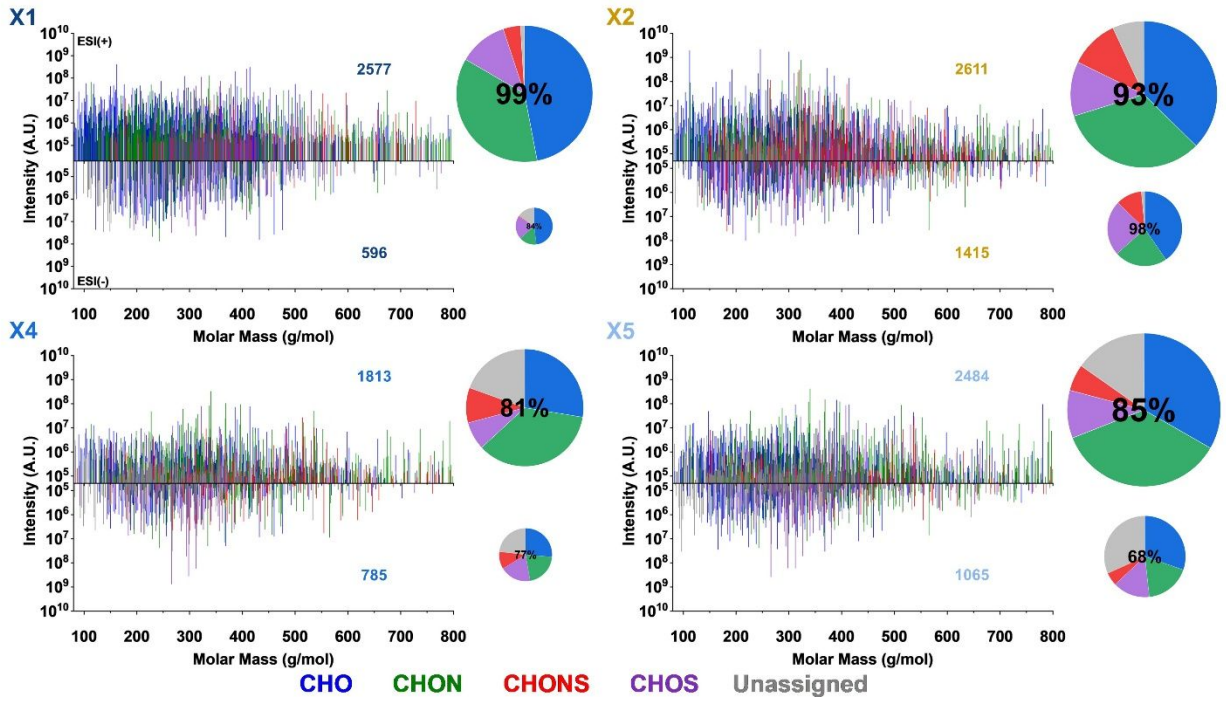

Figure 2. Representative mass spectra of four waste condensates acquired in ESI mode, where ESI(+) and ESI(−) intensities are plotted against positive and negative y-axis, respectively. Assigned peaks are plotted for neutral species, where the x-axis represents the molar mass (g/mol). The pie charts show color-coded relative fractions of different formula categories, and the sizes of pie charts are proportional to the numbers of detected species indicated by the numbers in each panel. The percent values in charts show fractions of the assigned MS peaks relative to the total number of detected peaks in each ionization mode dataset.

Color-coded pie chart inserts of Figure 2 show relative contributions CHO, CHON, CHOS, and CHONS groups of species detected by each of the ionization modes in four waste samples. Percent values of these contributions are summarized in Figure S2 of the supplemental information. CHO and CHON assigned species are the main components in all samples, accounting for more than half of the assignments. Condensate sample collected at the X2 site where a VE-based resin was used shows marginally larger fractions of CHON, compared to the samples from the other three sites. However, significantly higher fractions of CHOS and CHONS species (up to 35%) are observed in the X2 sample, compared to the X1-4-5 samples from the sites of S-based resin use. At these three sites, combined CHOS and CHONS contributions are largely at the level of ~20% or less. Most of the CHOS and CHONS species detected in the X2 sample contain enough oxygen atoms (> 4) to be possibly organosulfates (51% of total detected CHOS and CHONS), which is also consistent with their abundant detection in the ESI(−) mode, similar to literature reports.[63,64] Subsets of the identified organosulfates were additionally grouped according

to their projection along the -CH_2 Kendrick mass defect (KMD_{CH2}) vs. Kendrick mass space as shown in Figure S3 (Supplementary Note 5), similar to previously reported framework.[63] Differences between organosulfates identified in the X1-4-5 condensates (use of S-based resins) and the X2 condensate (use of VE-based resin) may indicate differences in the CHOS compounds formed during the accelerated reaction chemistry in microdroplets occurring from the evaporative drying and polymerization of waste components.[65] It is also likely that the resin material already contains CHONS and CHOS species.[66] However, these will still continue to react in the emission plume as the droplets evaporate. Overall, detected CHOS species are different for each of the samples (Figure S3), indicating different pathways of organosulfate formation. In addition, the nominal oxidation state of carbon (NOS_C) versus molar mass plots (Figure S4) show that only up to 28% of CHOS and CHONS species are significantly oxidized ($NOS_C > 0$) among all four of the samples, where there is no significant trend between the two resin types (Supplementary Note 6). Majority of CHOS and CHONS species exhibit values of $NOS_C < 0$ indicative of reduced species that can be easily oxidized in the presence of typical atmospheric pollutants (e.g., ozone, OH radical, NOx). Oxidation of these species will in turn increase their O/C ratios, reduce their volatility, and increase their viscosity, leading to the potential formation of solid EnvNP in the atmosphere.

A broad range of aliphatic and aromatic species were detected in each of the samples. Based on the assessment of characteristic DBE values (Figure S5), O/C and H/C ratios (Figure S6) of individual components, the S-based condensates (X1, 4-5) contain a large fraction of aliphatic functionalized (CHON, CHONS, and CHOS) compounds that are likely various co-products of the utilized commercial resin and initiator materials that are not involved in the intended formation of polystyrene (Supplementary Note 7). These functionalized compounds readily ionize in ESI mode,[37] as seen in Figure 2. The VE-based resin utilizes an aliphatic vinyl ester (i.e., tripropylene glycol diacrylate) monomer for intended polymerization. However, its corresponding X2 waste sample also contains a large fraction of aliphatic functionalized co-products. Remarkably, all waste condensates also contain unsaturated aromatic ($H/C < 1$) and highly oxidized aliphatic ($O/C > 0.5$) co-products. The aromatic compounds in the S-based samples (X1, 4-5) are possibly polymerization and oligomerization byproducts formed from the monomer styrene. The oxidized species in both resin types are likely derivatives of the resin materials and co-products present in high concentrations in commercial mixtures with chemical functionalities such as carboxylic acids,

ketones, aldehydes, esters, hemiacetals, or acetals as well as nitrogen and sulfur containing functional groups that formed during unintended side reactions. The extent of these side reactions cannot be fully apprehended as the complete chemical composition of the resin is unknown.

Figure 3 shows the distribution of calculated saturation mass concentrations (C_0) of waste condensate components,[34] summarized as box and whisker plots. The C_0 values of individual molecular components are presented in Figure S7 (Supplementary Note 8). Notably, components of all waste condensates cover a wide range of C_0 values from extremely low volatility organic compounds ($<10^{-4}$ μg m^{-3}) to highly volatile organic compounds ($>10^{6}$ μg m^{-3}), which would readily evaporate from drying droplets of the discharged steam laden waste. However, only 1% to 2% of the total number of identified compounds contributed to the VOC class. Most of the observed compounds (75-87%) fall into the semi-volatile (SVOC), low volatility (LVOC), or extremely low volatility (ELVOC) classes that will predominantly form OA and solid EnvNP particles. The remaining contribution is attributed to intermediate volatility (IVOC) class, which partitions between both gas- and particle- phases.[67]

The C_0 values of the monomer species used in two types of resins are 10^{7} μg m^{-3} (styrene, VOC class) and 10^{5} μg m^{-3} (tripropylene glycol diacrylate, IVOC class; VE-based resin),[68,69] which reflect contrasting VOC emissions from use of these two resins. However, while indeed the VE-based resin contains less VOC by mass than the S-based resin,[19] species found in the waste condensates show complex composition and common high contributions of SVOC, LVOC and ELVOC species in all four samples. Upon evaporation of water from the discharged waste droplets, these low-volatility species remain in the condensed phase forming oligomeric OA particles with viscoelastic properties of EnvNP.[9]

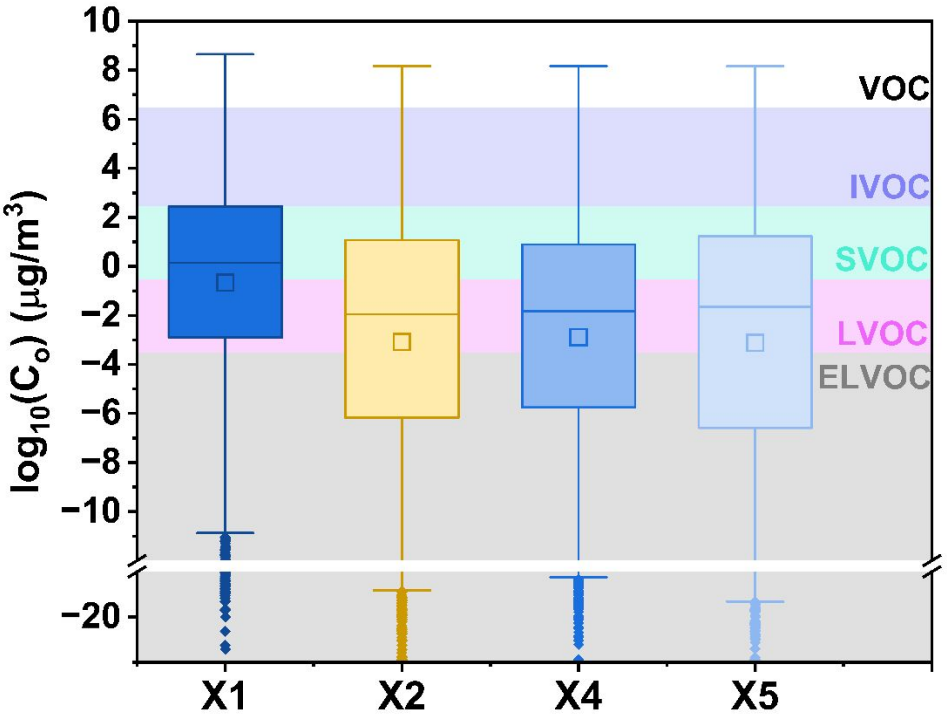

Figure 3. Summary of the saturation mass concentration ($log_{10}C_0$, μg m^{-3}) estimates of assigned species in each sample. Boxes enclose the interquartile range, the median values are indicated by the horizontal lines within the boxes, the mean values are indicated by the squares in the box, the whiskers extend to 1.5 of the interquartile range, and outliers beyond the whiskers are drawn with diamonds. The background colors indicate the volatility ranges of the organic compounds (OC) reported in Donahue et al. (2012)[33]: from top to bottom, volatile OC (VOC), intermediate-volatility OC (IVOC), semi volatile OC (SVOC), low-volatility OC (LVOC), and extremely low volatility VOC (ELVOC).

Figure 4 illustrates estimated fractions of the gas-particle partitioning calculated for the components of waste condensate samples, if they were aerosolized at different total mass loadings. The estimates utilized the volatility basis set (VBS) framework[70] which bins individual species based on their C_0 values into a set of logC* bins of integer values, and then calculates gas-particle mass ratios in each of the individual bins (Supplementary note 9). Figure 4 shows summary plots of the total mass ratios summed over all bins, the extended VBS distributions over broad range of logC* bins are included in Figures S9-S11. While exact fluxes of the organic waste discharged in the air at the emission sources and dilution dynamics remain ambiguous, the VBS estimates suggest that the condensed-phase mass fractions would be more than 70% of the aerosol-gas mixture assuming even modest air pollution concentrations with ~100 μg m^{-3} of the total mass loadings. Even after significant dilution of the emission plumes down to ~1 μg m^{-3}, 50-60% of the

air-discharged waste would remain in the condensed phase or airborne particles composed mostly of the ELVOC components.

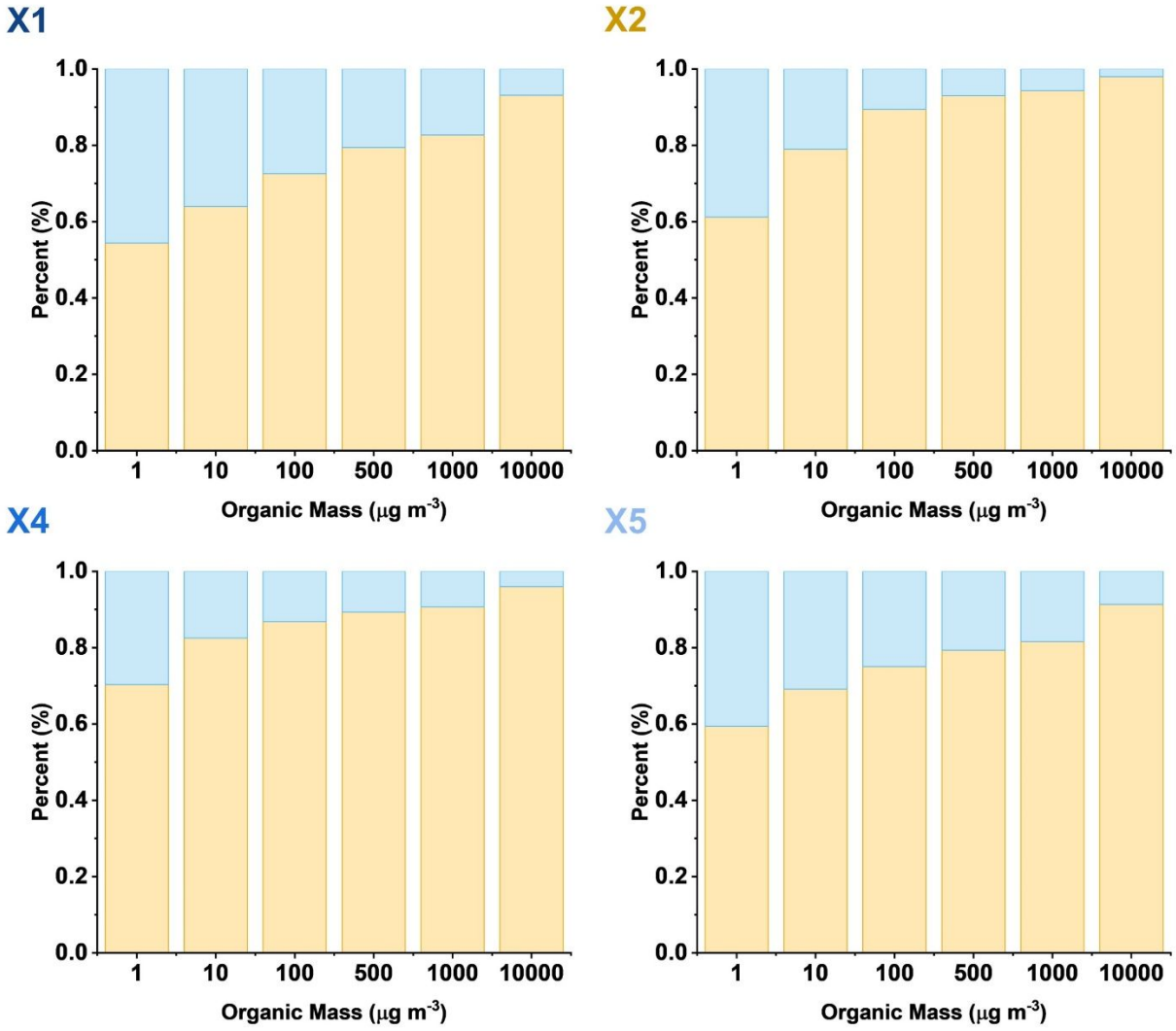

Figure 4. Estimates of the gas-particle partitioning of individual waste condensate components based on the volatility basis set (VBS) framework. The stacked bars represent fractions of the waste condensate organic material partitioning between gas (blue color) and particle phases (yellow color) when aerosolized at different total organic mass loadings shown on the X-axis.

Figure 5 shows the box and whisker distribution plots showing summary of the viscosity values (η, Pa s) calculated for identified components of four waste mixtures.[32] The corresponding

glass transition temperatures (T_g) and all η values of individual molecular components are shown in Figures S12 and S13, respectively (Supplementary Note 10). In addition to saturation mass concentrations (C_0), viscosity values inform a predictive understanding of how individual species would impact OA formation and growth, their phase state, chemical reactivity, and hygroscopic properties.[71,72] Consistently with the C_0 values reported above, Figure 5 indicates that either viscous, semi-solid ($\eta>10^2$ Pa s) or hard solid ($\eta>10^{12}$ Pa s) viscoelastic properties are expected for OA particles formed after evaporation of water from aerosolized waste condensate. Specifically, components of X2, X4, and X5 samples are heavily shifted towards the maximum value (10^{15} Pa s), and the upper 75% of the distribution falls into the high end of semi-solid and solid ranges. Compounds containing the aforementioned functional groups (e.g., carboxylic acids, ketones, aldehydes, esters, hemiacetals, or acetals) can undergo reactions, such as esterification, aldol condensation, or Schiff base formation, that produce oligomeric compounds during droplet evaporation with low volatilities and high viscosities, such as EnvNP particles.[9,73–80]

According to available public records, a significant amount of resin, ranging from 61 to 454 tons, is typically used in CIPP projects in urban areas of the US.[4] Laboratory studies indicate that approximately 9% of the organic resin material is released into the air. [4] This translates to over 5 tons of the organic chemical waste discharged in the air per project, posing potential environmental and health concerns. Experimental estimates[9] of the EnvNP fractions of only 5% of the total organic waste, yield 0.25 tons of EnvNP per project. However, the specific impact of these particle emissions on urban pollution is not well-documented, and their consideration has been largely overlooked in previous studies. Thus, systematic lab studies investigating the gas-phase and condensed phase emissions and their influence on OA and EnvNP formation are necessary.[9]

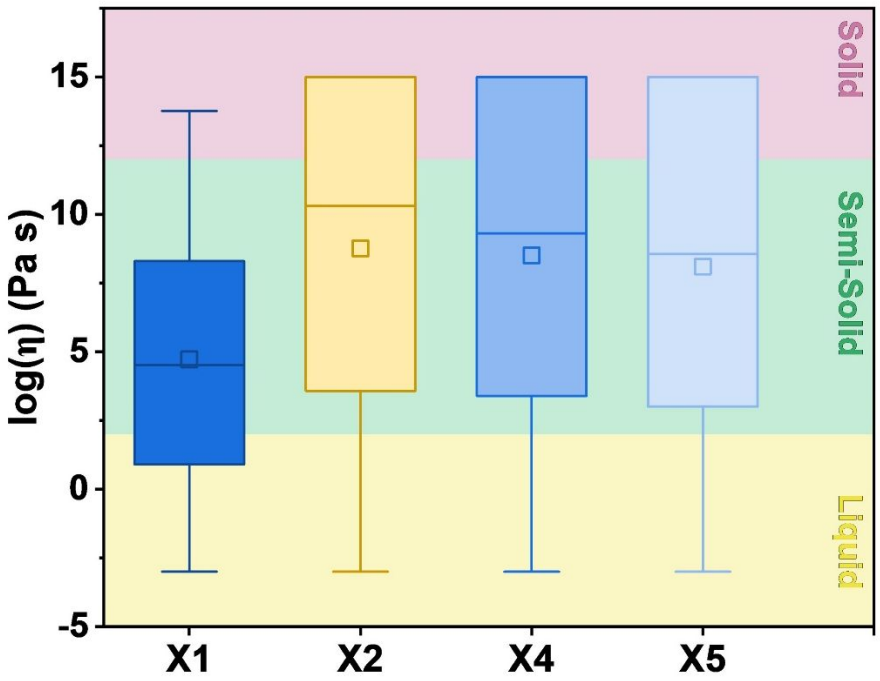

Figure 5. Summary of estimated viscosity log(η) values of species detected in the four waste condensates. Box encloses the interquartile range, the median values are indicated by the horizontal lines within the boxes, the mean values are indicated by the squares in the boxes, the whiskers extend to 1.5 of the interquartile range. The background colors indicate the viscosity ranges reported in Koop et al. (2011):[71] from top to bottom, solid, semi-solid, and liquid.

Untargeted chemical characterization of the waste condensates shows a very complex mixture of organic components, which cannot be practically quantified on the single-component basis for all of them. For targeted analysis, specific selections need to be made for quantitative measurements of certain species of interest, such as targeted detection of controlled toxicants,[4,5,17,19] detection of selected species governing formation of EnvNP particles,[9] detection of fingerprint species for the source apportionment of waste emissions, etc. In this work, we quantify concentrations of several known pollutants previously detected in the CIPP waste samples.[4,17,19] Figure 6 illustrates seven selected species and their corresponding extracted ion chromatograms recorded for each of the waste condensates. The list of species includes: (1) benzoic acid, (2) methyl methacrylate, (3) benzaldehyde, (4) acetophenone, (5) tripropylene glycol diacrylate, and (6) dibutyl phthalate. Benzaldehyde and benzoic acid are oxidation products of styrene and initiators, acetophenone is a decomposition product of the peroxide initiator, methyl methacrylate and tripropylene glycol diacrylate are polymer monomers, and dibutyl phthalate is a

plasticizer.[19] The selected species were quantified using the integrated peak areas of the extracted ion chromatograms (EIC) recorded in the ESI(+) mode. Details of the calibration experiments and the corresponding data analysis are summarized in Supplementary Note 11, including the calibration curves (Figure S14) and absorbance spectra (Figure S15). The limits of detection and quantitation based on the calibration curves (Figure S14) are included as Table S2. Figure 7 shows concentrations of these targeted species quantified in each of the waste condensates summarized as a histogram, while their numerical values are also included in Table 1 together with the corresponding risk-based SL values recommended by EPA.[36]

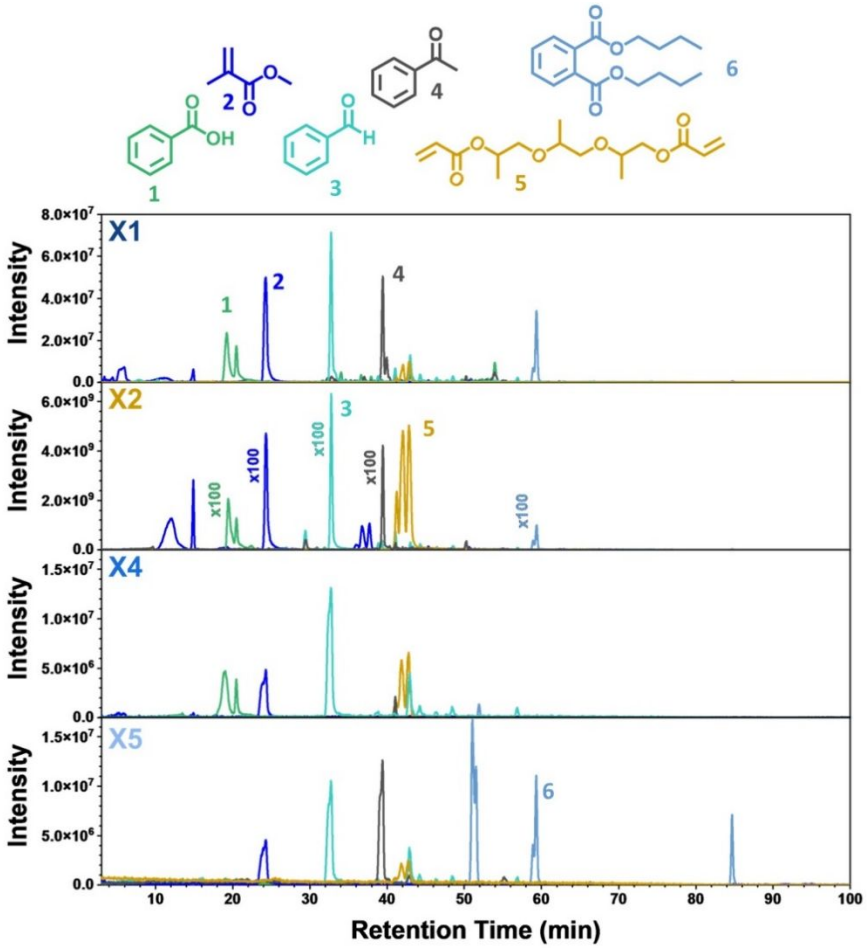

Figure 6. Extracted ion chromatograms (EIC) for selected resin components recorded in ESI(+) mode in four waste condensates of this study. Structures are numbered in order of their retention times: benzoic acid (1), methyl methacrylate (2), benzaldehyde (3), acetophenone (4), tripropylene glycol diacrylate (5), and dibutyl phthalate (6). Selected extracted chromatograms were scaled by a factor of x100 shown in the plot. Multiple EIC peaks at different retention times indicate the existence of different isomers with the same elemental formulars.

Measured concentrations of the selected target compounds show that many of them are somewhat comparable between the waste samples, regardless of whether S-based or VE-based resins were used at the operation site. However, the concentration of tripropylene glycol diacrylate, the vinyl ester monomer of the VE-based resins, is remarkably higher (~20 mg L^{-1}) in the corresponding X2 waste sample, than its levels (0.005-0.02 mg L^{-1}) in the X1-4-5 samples. Additionally, when the TOC concentration values measured in the X2 samples of 133.40 mg L^{-1} are higher versus 13.18-53.76 mg L^{-1} reported for the X1-4-5 samples. This suggests that while use of the VE-based resin eliminates high emissions of the gas-phase constituents, on the other hand it increases amount of the condensed-phase organic waste. This substantial increase in the condensed-phase waste will translate in higher mass loadings of OA and EnvNP particles emitted at the sites of VE-based resin operation. Concentrations of the quantified species exceed values of the carcinogenic SL and on par with the noncarcinogenic SL recommended by EPA for groundwater protection.[36] Therefore, disposal of these collected condensates would require appropriate treatment before it can be safely discharged in sewers. Substances with high $\log K_{OW}$ values (between 3–14) are of concern as they are assumed to absorb into organic matter more readily in soils or sediments because of their low affinity for water with a greater potential to bioconcentration and biomagnification in living organism.[81] Butylated hydroxytoluene ($\log K_{OW}$ = 5.1) and dibutyl phthalate ($\log K_{OW}$ = 4.5) present significant risks if present in ground water.[36] Airborne discharge of the microdroplets containing these components is even of higher concern with respect to plausible health effects of these emissions. Of particular concern are elevated concentrations of benzaldehyde, which is a known irritant and possible carcinogen.[82] Additionally, butylated hydroxytoluene, which is known to decrease liver and kidney function and is associated with toxic effects in lung tissue,[83] was also found to the waste mixture at the level exceed in the carcinogenic SL value recommended by EPA.[36] Previous studies and firsthand observations by some authors have indicated that CIPP workers did not always wear personal protective equipment and therefore could be possibly exposed to unknown levels of aerosolized pollutants upon droplet evaporation, which were noted as visible fine powder EnvNP residues deposited on trees near waste discharge points.[4] It follows that systematic assessment of organic pollutants emitted as both gas- and condensed-phase species is needed for safe operations at the installation sites, regardless of type of the resin being used.

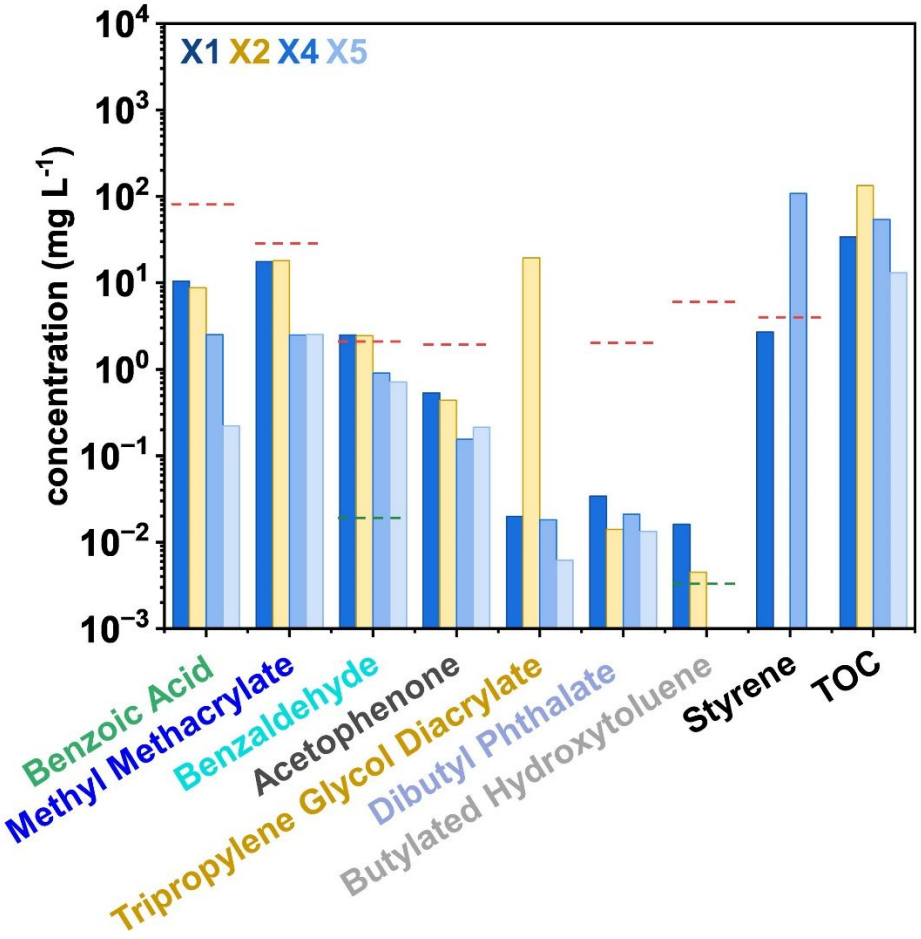

Figure 7. Concentrations of selected pollutants in the waste condensates collected at installation sites. Risk-based EPA recommended screening levels (SL) established for groundwater protection[36] are shown for comparison as the horizontal red (noncarcinogenic SL) and green (carcinogenic SL) dashed lines.

Conclusions

Previous studies quantifying emissions from trenchless pipe repair operation have focused solely on the gas-phase pollutants. However, a much more complex multiphase waste mixture is released in this operation. This study is the first to highlight the importance and complexity of the condensed phase organic species found in the field collected waste condensates. Systematic follow-up studies should quantify aerosol size distributions and their atmospheric concentrations, including targeted quantitative analysis of a broad range of the condensed particle-phase species containing resin components, initiators, oligomerization byproducts, PAHs and their derivatives. For many of them, the airborne condensed waste concentrations may exceed safe exposure levels that also need to be established. The low volatilities and high viscosities of the organic species

found in the waste condensates imply they will enhance emissions of organic aerosol at the sites, while fraction of them may form airborne EnvNP particles.[9]

To mitigate effects of the associated air pollution and provide better protection for workers at the installation sites, critical assessment of the toxicological impacts of these emissions is very much needed. Future studies should focus on both gas- and condensed-phase emissions. Systematic experimental studies need be conducted to investigate the impact of resin type, initiators, and curing conditions on the amount of discharged waste considering both gas- and condensed-phase organic pollutants. Physiochemical properties and compositional differences may be observed during a single CIPP's manufacture, from resin to hard plastic. We note that samples investigated in this study were collected at various selected periods of CIPP installation and they only exemplify complexity of the emissions rather than generalize airborne emission of the entire CIPP manufacture technology, which employ different composites of resin and various curing procedures. These differences alter composition and mass loadings of the aerosolized emissions which need to be studied in systematic field studies. Furthermore, the chemical composition of the resin material itself should be explored in more detail. This composition should be compared to that of the discharged waste to understand reaction mechanisms. A more detailed understanding of the extent of unintended oligomerization and aerosol formation occurring in the drying waste plume is also recommended.

Acknowledgements

This work was supported by the U.S. National Science Foundation, Grants No. CBET-1624183, -2129166 (AW group) and No. CBET-2107946 (AL group), the National Science Foundation Graduate Research Fellowship Program, Grant No. DGE-1333468 (ACM), the Purdue University Bilsland graduate school dissertation fellowship (CPW), and the Purdue University Ross Fellowship program (BNP, YN). We would like to acknowledge S.M.T. Sendesi, B. E. Boor, and J.A. Howarter for their field work collecting waste samples used in this study. Any opinions, findings, and conclusions or recommendations expressed in this material are those of the author(s) and do not necessarily reflect the views of the National Science Foundation.

Author Contributions Statement

A. C. M. and A. L. designed the overall project framework and experiments. A. C. M. performed the LC separations and method development protocols. A. C. M., C. P. W., and B. N. P. performed the molecular characterization experiments and processed, analyzed, and interpreted the HPLC-PDA-HRMS datasets. Y. N. conducted bulk and GC-MS analysis of the waste condensates. A. C. M. and A. L. wrote the manuscript with contributions from all co-authors. A.J.W. and A.L. secured grant support for this study and managed the project.

References

1 *Cured-In-Place Pipe (CIPP) Market Size, Share, Trend, Forecast, & Competitive Analysis: 2020-2025*, Stratview Research, 2019.

2 E. Matthews, J. Matthews and S. Eklund, *NASSCO CIPP Emissions Phase 2: Evaluation of Air Emissions from Polyester Resin CIPP with Steam Cure Final Report*, 2020.

3 B. C. McDonald, D. R. Gentner, A. H. Goldstein and R. A. Harley, Long-Term Trends in Motor Vehicle Emissions in U.S. Urban Areas, *Environ. Sci. Technol.*, 2013, **47**, 10022–10031.

4 S. M. Teimouri Sendesi, K. Ra, E. N. Conkling, B. E. Boor, Md. Nuruddin, J. A. Howarter, J. P. Youngblood, L. M. Kobos, J. H. Shannahan, C. T. Jafvert and A. J. Whelton, Worksite Chemical Air Emissions and Worker Exposure during Sanitary Sewer and Stormwater Pipe Rehabilitation Using Cured-in-Place-Pipe (CIPP), *Environ. Sci. Technol. Lett.*, 2017, **4**, 325–333.

5 K. Ra, S. M. Teimouri Sendesi, Md. Nuruddin, N. N. Zyaykina, E. N. Conkling, B. E. Boor, C. T. Jafvert, J. A. Howarter, J. P. Youngblood and A. J. Whelton, Considerations for emission monitoring and liner analysis of thermally manufactured sewer cured-in-place-pipes (CIPP), *J. Hazard. Mater.*, 2019, **371**, 540–549.

6 E. B. Ajdari, University of New Orleans, 2016.

7 E. Matthews, J. Kraft, G. Hossain, A. Bednar, C. Laber, S. Alam, T. Manzur, J. Matthews, J. Howell and S. Eklund, Air Quality Dispersion Modelling to Evaluate CIPP Installation Styrene Emissions, *Int. J. Environ. Res. Public. Health*, 2022, **19**, 13800.

8 K. Ra, S. M. Teimouri Sendesi, J. A. Howarter, C. T. Jafvert, B. M. Donaldson and A. J. Whelton, Critical Review: Surface Water and Stormwater Quality Impacts of Cured-In-Place Pipe Repairs, *Am. Water Works Assoc.*, 2018, **110**, 15–32.

9 A. C. Morales, J. M. Tomlin, C. P. West, F. A. Rivera-Adorno, B. N. Peterson, S. A. L. Sharpe, Y. Noh, S. M. T. Sendesi, B. E. Boor, J. A. Howarter, R. C. Moffet, S. China, B. T. O'Callahan, P. Z. El-Khoury, A. J. Whelton and A. Laskin, Atmospheric emission of nanoplastics from sewer pipe repairs, *Nat. Nanotechnol.*, 2022, **17**, 1171–1177.

10 Y. Noh, J. H. Shannahan, A. G. Hoover, K. G. Pennell, M. H. Weir and A. J. Whelton, Bystander Chemical Exposures and Injuries Associated With Nearby Plastic Sewer Pipe Manufacture: Public Health Practice and Lessons, *J. Environ. Health*, 2022, **85**, 22–31.

11 L. Kobos, S. M. Teimouri Sendesi, A. J. Whelton, B. E. Boor, J. A. Howarter and J. Shannahan, *In vitro* toxicity assessment of emitted materials collected during the manufacture of water pipe plastic linings, *Inhal. Toxicol.*, 2019, **31**, 131–146.

12 M. L. Tabor, D. Newman and A. J. Whelton, Stormwater Chemical Contamination Caused by Cured-in-Place Pipe (CIPP) Infrastructure Rehabilitation Activities, *Environ. Sci. Technol.*, 2014, **48**, 10938–10947.

13 R. F. LeBouf, D. A. Burns, A. Ranpara and L. M. Kobos, *Evaluation of exposures to styrene during cured-in-place pipe liner preparation and during pipe repairs using hot water and steam.*, U.S. Department of Health and Human Services, Public Health Service, Centers for Disease Control and Prevention, National Institute for Occupational Safety and Health, 2021.

14 R. F. LeBouf and D. A. Burns, *Evaluation of Exposures to Styrene During Ultraviolet Cured-in-place Pipe Installation*, U.S. Department of Health and Human Services Centers for Disease Control and Prevention National Institute for Occupational Safety and Health, 2019.

15 R. F. LeBouf and D. A. Burns, *Health Hazard Evaluation Report: Evaluation of Exposures to Styrene During Ultraviolet Cured-in- Place-Pipe Installation.*, Centers for Disease Control and Prevention, U.S. National Institute of Occupational Safety and Health, Morgantown, WV, 2019.

16 Y. Noh, B. E. Boor, J. H. Shannahan, C. D. Troy, C. T. Jafvert and A. J. Whelton, Emergency responder and public health considerations for plastic sewer lining chemical waste exposures in indoor environments, *J. Hazard. Mater.*, 2022, **422**, 126832.

17 S. M. Teimouri Sendesi, Y. Noh, M. Nuruddin, B. E. Boor, J. A. Howarter, J. P. Youngblood, C. T. Jafvert and A. J. Whelton, An emerging mobile air pollution source: outdoor plastic liner manufacturing sites discharge VOCs into urban and rural areas, *Environ. Sci. Process. Impacts*, 2020, **22**, 1828–1841.

18 Y. Noh, L. Xia, N. N. Zyaykina, B. E. Boor, J. H. Shannahan and A. J. Whelton, Regulatory Significance of Plastic Manufacturing Air Pollution Discharged into Terrestrial Environments and Real-Time Sensing Challenges, *Environ. Sci. Technol. Lett.*, 2023, acs.estlett.2c00710.

19 Y. Noh, T. Odimayomi, S. M. Teimouri Sendesi, J. P. Youngblood and A. J. Whelton, Environmental and human health risks of plastic composites can be reduced by optimizing manufacturing conditions, *J. Clean. Prod.*, 2022, **356**, 131803.

20 M. Nuruddin, G. P. Mendis, K. Ra, S. M. T. Sendesi, T. Futch, J. Goodsell, A. J. Whelton, J. P. Youngblood and J. A. Howarter, Evaluation of the physical, chemical, mechanical, and thermal properties of steam-cured PET/polyester cured-in-place pipe, *J. Compos. Mater.*, 2019, **53**, 2687–2699.

21 J. E. McAlvin, Green Composites Through the Use of Styrene-Free Resins and Unsaturated Polyesters Derived from Renewable and Recycled Raw Materials, *Compos. Febr.*, 2011, 2–4.

22 W. Moore and N.-N. Dig, Non-styrene options for cured in place pipe, *NASTT No Dig Febr.*

23 X. Li, K. Ra, M. Nuruddin, S. M. Teimouri Sendesi, J. A. Howarter, J. P. Youngblood, N. Zyaykina, C. T. Jafvert and A. J. Whelton, Outdoor manufacture of UV-Cured plastic linings for storm water culvert repair: Chemical emissions and residual, *Environ. Pollut.*, 2019, **245**, 1031–1040.

24 PMW Technologies LLC, *EnviroSnap Resin Series Best Practices Guide*, 2020.

25 R. K. Lee, *Risks associated with CIPP lining of storm water pipes and the release of styrene*, 2008.

26 C. Baley, Y. Perrot, P. Davies, A. Bourmaud and Y. Grohens, Mechanical Properties of Composites Based on Low Styrene Emission Polyester Resins for Marine Applications, *Appl. Compos. Mater.*, 2006, **13**, 1–22.

27 X. Cao and L. J. Lee, Control of shrinkage and residual styrene of unsaturated polyester resins cured at low temperatures: I. Effect of curing agents, *Polymer*, 2003, **44**, 1893–1902.

28 P. Compston, J. Schiemer and A. Cvetanovska, Mechanical properties and styrene emission levels of a UV-cured glass-fibre/vinylester composite, *Compos. Struct.*, 2008, **86**, 22–26.

29 M. Najafi, M. Sattler, K. Schug, V. Kaushal, S. Korky, G. Iyer, S. Kakkera and S. Habibzadek, *Evaluation of Potential Release of Organic Chemicals in the Steam Exhaust and Other Release Points during Pipe Rehabilitation Using the Trenchless Cured-In-Place Pipe (CIPP) Method*, National Association of Software and Service Companies (NASSCO), 2018.

30 Agency for Toxic Substances and Disease Registry, 2007.

31 Z. Hong, M. Li, H. Wang, L. Xu, Y. Hong, J. Chen, J. Chen, H. Zhang, Y. Zhang, X. Wu, B. Hu and M. Li, Characteristics of atmospheric volatile organic compounds (VOCs) at a mountainous forest site and two urban sites in the southeast of China, *Sci. Total Environ.*, 2019, **657**, 1491–1500.

32 W.-S. W. DeRieux, Y. Li, P. Lin, J. Laskin, A. Laskin, A. K. Bertram, S. A. Nizkorodov and M. Shiraiwa, Predicting the glass transition temperature and viscosity of secondary organic material using molecular composition, *Atmospheric Chem. Phys.*, 2018, **18**, 6331–6351.

33 N. M. Donahue, J. H. Kroll, S. N. Pandis and A. L. Robinson, A two-dimensional volatility basis set–Part 2: Diagnostics of organic-aerosol evolution, *Atmospheric Chem. Phys.*, 2012, **12**, 615–634.

34 Y. Li, U. Pöschl and M. Shiraiwa, Molecular corridors and parameterizations of volatility in the chemical evolution of organic aerosols, *Atmospheric Chem. Phys.*, 2016, **16**, 3327–3344.

35 *United States Environmental Protection Agency (USEPA). Method 415.1. Organic Carbon, Total (Combustion or Oxidation)*, United States Environmental Protection Agency: Washington, DC, USA, 1974.

36 *Regional Screening Level (RSL) Resident Soil to Groundwater Table*, US Environmental Protection Agency, 2022.

37 P. Lin, L. T. Fleming, S. A. Nizkorodov, J. Laskin and A. Laskin, Comprehensive Molecular Characterization of Atmospheric Brown Carbon by High Resolution Mass Spectrometry with Electrospray and Atmospheric Pressure Photoionization, *Anal. Chem.*, 2018, **90**, 12493–12502.

38 P. Lin, N. Bluvshtein, Y. Rudich, S. A. Nizkorodov, J. Laskin and A. Laskin, Molecular Chemistry of Atmospheric Brown Carbon Inferred from a Nationwide Biomass Burning Event, *Environ. Sci. Technol.*, 2017, **51**, 11561–11570.

39 A. P. S. Hettiyadura, V. Garcia, C. Li, C. P. West, J. Tomlin, Q. He, Y. Rudich and A. Laskin, Chemical Composition and Molecular-Specific Optical Properties of Atmospheric Brown Carbon Associated with Biomass Burning, *Environ. Sci. Technol.*, 2021, **55**, 2511–2521.

40 A. P. S. Hettiyadura and A. Laskin, Quantitative analysis of polycyclic aromatic hydrocarbons using high-performance liquid chromatography-photodiode array-high-resolution mass spectrometric detection platform coupled to electrospray and atmospheric pressure photoionization sources, *J. Mass Spectrom.*, 2022, **57**, e4804.

41 C. P. West, A. P. S. Hettiyadura, A. Darmody, G. Mahamuni, J. Davis, I. Novosselov and A. Laskin, Molecular Composition and the Optical Properties of Brown Carbon Generated by the Ethane Flame, *ACS Earth Space Chem.*, 2020, **4**, 1090–1103.

42 D. B. Robb and M. W. Blades, State-of-the-art in atmospheric pressure photoionization for LC/MS, *Anal. Chim. Acta*, 2008, **627**, 34–49.

43 T. Pluskal, S. Castillo, A. Villar-Briones and M. Orešič, MZmine 2: Modular framework for processing, visualizing, and analyzing mass spectrometry-based molecular profile data, *BMC Bioinformatics*, 2010, **11**, 395.

44 O. D. Myers, S. J. Sumner, S. Li, S. Barnes and X. Du, One Step Forward for Reducing False Positive and False Negative Compound Identifications from Mass Spectrometry Metabolomics Data: New Algorithms for Constructing Extracted Ion Chromatograms and Detecting Chromatographic Peaks, *Anal. Chem.*, 2017, **89**, 8696–8703.

45 P. J. Roach, J. Laskin and A. Laskin, Higher-Order Mass Defect Analysis for Mass Spectra of Complex Organic Mixtures, *Anal. Chem.*, 2011, **83**, 4924–4929.

46 Y. Zhou, C. P. West, A. P. S. Hettiyadura, X. Niu, H. Wen, J. Cui, T. Shi, W. Pu, X. Wang and A. Laskin, Measurement report: Molecular composition, optical properties, and radiative effects of water-soluble organic carbon in snowpack samples from northern Xinjiang, China, *Atmospheric Chem. Phys.*, 2021, **21**, 8531–8555.

47 P. Lin, A. G. Rincon, M. Kalberer and J. Z. Yu, Elemental Composition of HULIS in the Pearl River Delta Region, China: Results Inferred from Positive and Negative Electrospray High Resolution Mass Spectrometric Data, *Environ. Sci. Technol.*, 2012, **46**, 7454–7462.

48 K. Wang, Y. Zhang, R.-J. Huang, J. Cao and T. Hoffmann, UHPLC-Orbitrap mass spectrometric characterization of organic aerosol from a central European city (Mainz, Germany) and a Chinese megacity (Beijing), *Atmos. Environ.*, 2018, **189**, 22–29.

49 Y. Zhou, C. P. West, A. P. S. Hettiyadura, W. Pu, T. Shi, X. Niu, H. Wen, J. Cui, X. Wang and A. Laskin, Molecular Characterization of Water-Soluble Brown Carbon Chromophores in Snowpack from Northern Xinjiang, China, *Environ. Sci. Technol.*, 2022, **56**, 4173–4186.

50 F. W. McLafferty, F. Tureček and F. Turecek, *Interpretation of mass spectra*, University science books, 1993.

51 B. P. Koch and T. Dittmar, From mass to structure: an aromaticity index for high-resolution mass data of natural organic matter, *Rapid Commun. Mass Spectrom.*, 2006, **20**, 926–932.

52 B. P. Koch and T. Dittmar, From mass to structure: an aromaticity index for high-resolution mass data of natural organic matter, *Rapid Commun. Mass Spectrom.*, 2016, **30**, 250–250.

53 J. H. Kroll, N. M. Donahue, J. L. Jimenez, S. H. Kessler, M. R. Canagaratna, K. R. Wilson, K. E. Altieri, L. R. Mazzoleni, A. S. Wozniak, H. Bluhm, E. R. Mysak, J. D. Smith, C. E. Kolb and D. R. Worsnop, Carbon oxidation state as a metric for describing the chemistry of atmospheric organic aerosol, *Nat. Chem.*, 2011, **3**, 133–139.

54 J. H. Kroll, C. Y. Lim, S. H. Kessler and K. R. Wilson, Heterogeneous oxidation of atmospheric organic aerosol: Kinetics of changes to the amount and oxidation state of particle-phase organic carbon, *J. Phys. Chem. A*, 2015, **119**, 10767–10783.

55 T. Ghislain, P. Faure and R. Michels, Detection and Monitoring of PAH and Oxy-PAHs by High Resolution Mass Spectrometry: Comparison of ESI, APCI and APPI Source Detection, *J. Am. Soc. Mass Spectrom.*, 2012, **23**, 530–536.

56 W. C. Hockaday, J. M. Purcell, A. G. Marshall, J. A. Baldock and P. G. Hatcher, Electrospray and photoionization mass spectrometry for the characterization of organic matter in natural waters: a qualitative assessment: Characterization of organic matter in natural waters, *Limnol. Oceanogr. Methods*, 2009, **7**, 81–95.

57 H. Deng, P. S. J. Lakey, Y. Wang, P. Li, J. Xu, H. Pang, J. Liu, X. Xu, X. Li, X. Wang, Y. Zhang, M. Shiraiwa and S. Gligorovski, Daytime SO_2 chemistry on ubiquitous urban surfaces as a source of organic sulfur compounds in ambient air, *Sci. Adv.*, 2022, **8**, eabq6830.

58 R. Volkamer, J. L. Jimenez, F. San Martini, K. Dzepina, Q. Zhang, D. Salcedo, L. T. Molina, D. R. Worsnop and M. J. Molina, Secondary organic aerosol formation from anthropogenic air pollution: Rapid and higher than expected, *Geophys. Res. Lett.*, 2006, **33**, L17811.

59 N. Sareen, E. M. Waxman, B. J. Turpin, R. Volkamer and A. G. Carlton, Potential of Aerosol Liquid Water to Facilitate Organic Aerosol Formation: Assessing Knowledge Gaps about Precursors and Partitioning, *Environ. Sci. Technol.*, 2017, **51**, 3327–3335.

60 W. Jiang, M. V. Misovich, A. P. S. Hettiyadura, A. Laskin, A. S. McFall, C. Anastasio and Q. Zhang, Photosensitized Reactions of a Phenolic Carbonyl from Wood Combustion in the Aqueous Phase—Chemical Evolution and Light Absorption Properties of AqSOA, *Environ. Sci. Technol.*, 2021, **55**, 5199–5211.

61 M. M. H. El-Sayed, Y. Wang and C. J. Hennigan, Direct atmospheric evidence for the irreversible formation of aqueous secondary organic aerosol: irreversible atmospheric AqSOA formation, *Geophys. Res. Lett.*, 2015, **42**, 5577–5586.

62 B. Ervens, B. J. Turpin and R. J. Weber, Secondary organic aerosol formation in cloud droplets and aqueous particles (aqSOA): a review of laboratory, field and model studies, *Atmospheric Chem. Phys.*, 2011, **11**, 11069–11102.

63 S. L. Blair, A. C. MacMillan, G. T. Drozd, A. H. Goldstein, R. K. Chu, L. Paša-Tolić, J. B. Shaw, N. Tolić, P. Lin, J. Laskin, A. Laskin and S. A. Nizkorodov, Molecular Characterization of Organosulfur Compounds in Biodiesel and Diesel Fuel Secondary Organic Aerosol, *Environ. Sci. Technol.*, 2017, **51**, 119–127.

64 S. Tao, X. Lu, N. Levac, A. P. Bateman, T. B. Nguyen, D. L. Bones, S. A. Nizkorodov, J. Laskin, A. Laskin and X. Yang, Molecular Characterization of Organosulfates in Organic Aerosols from Shanghai and Los Angeles Urban Areas by Nanospray-Desorption Electrospray Ionization High-Resolution Mass Spectrometry, *Environ. Sci. Technol.*, 2014, **48**, 10993–11001.

65 L. Qiu and R. G. Cooks, Simultaneous and Spontaneous Oxidation and Reduction in Microdroplets by the Water Radical Cation/Anion Pair, *Angew. Chem.*, , DOI:10.1002/ange.202210765.

66 B. N. Peterson, A. C. Morales, J. M. Tomlin, C. G. W. Gorman, P. E. Christ, S. A. L. Sharpe, S. M. Huston, F. A. Rivera-Adorno, B. T. O'Callahan, M. Fraund, Y. Noh, P. Pahari, A. J. Whelton, P. Z. El-Khoury, R. C. Moffet, A. Zelenyuk and A. Laskin, Chemical Characterization of Nanoplastic Particles Formed in Airborne Waste Discharged from Sewer Pipe Repairs, *Environ. Sci. Process. Impacts*.

67 A. Hodzic, J. L. Jimenez, S. Madronich, M. R. Canagaratna, P. F. DeCarlo, L. Kleinman and J. Fast, Modeling organic aerosols in a megacity: potential contribution of semi-volatile and intermediate volatility primary organic compounds to secondary organic aerosol formation, *Atmospheric Chem. Phys.*, 2010, **10**, 5491–5514.

68 IARC Working Group on the Evaluation of Carcinogenic Risks to Humans, *Exposure Data*, International Agency for Research on Cancer, 2019.

69 Tripropyleneglycol diacrylate, Toxicological Evaluation and Limit Values for 2-Ethylhexyl acrylate, Propylene carbonate, Quaternary ammonium compounds, Triglycidyl isocyanurate, and Tripropyleneglycol diacrylate, https://www2.mst.dk/udgiv/publications/2000/87-7944-210-2/html/kap06_eng.htm.

70 N. M. Donahue, A. L. Robinson and S. N. Pandis, Atmospheric organic particulate matter: From smoke to secondary organic aerosol, *Atmos. Environ.*, 2009, **43**, 94–106.

71 T. Koop, J. Bookhold, M. Shiraiwa and U. Pöschl, Glass transition and phase state of organic compounds: dependency on molecular properties and implications for secondary organic aerosols in the atmosphere, *Phys. Chem. Chem. Phys.*, 2011, **13**, 19238.

72 N. E. Rothfuss and M. D. Petters, Influence of Functional Groups on the Viscosity of Organic Aerosol, *Environ. Sci. Technol.*, 2017, **51**, 271–279.

73 H. Kimura, A simple method for the anionic polymerization of α-carbonyl acids in water, *J. Polym. Sci. Part Polym. Chem.*, 1998, **36**, 189–193.

74 P. J. Ziemann, Formation of alkoxyhydroperoxy aldehydes and cyclic peroxyhemiacetals from reactions of cyclic alkenes with O3 in the presence of alcohols, *J. Phys. Chem. A*, 2003, **107**, 2048–2060.

75 T. B. Nguyen, P. J. Roach, J. Laskin, A. Laskin and S. A. Nizkorodov, Effect of humidity on the composition of isoprene photooxidation secondary organic aerosol, *Atmospheric Chem. Phys.*, 2011, **11**, 6931–6944.

76 R. Zhao, A. K. Y. Lee, R. Soong, A. J. Simpson and J. P. D. Abbatt, Formation of aqueous-phase α-hydroxyhydroperoxides (α-HHP): potential atmospheric impacts, *Atmospheric Chem. Phys.*, 2013, **13**, 5857–5872.

77 H. Herrmann, T. Schaefer, A. Tilgner, S. A. Styler, C. Weller, M. Teich and T. Otto, Tropospheric Aqueous-Phase Chemistry: Kinetics, Mechanisms, and Its Coupling to a Changing Gas Phase, *Chem. Rev.*, 2015, **115**, 4259–4334.

78 J. Laskin, A. Laskin, S. A. Nizkorodov, P. Roach, P. Eckert, M. K. Gilles, B. Wang, H. J. (Julie) Lee and Q. Hu, Molecular Selectivity of Brown Carbon Chromophores, *Environ. Sci. Technol.*, 2014, **48**, 12047–12055.

79 S. S. Petters, T. G. Hilditch, S. Tomaz, R. E. H. Miles, J. P. Reid and B. J. Turpin, Volatility Change during Droplet Evaporation of Pyruvic Acid, *ACS Earth Space Chem.*, 2020, **4**, 741–749.

80 T. B. Nguyen, P. B. Lee, K. M. Updyke, D. L. Bones, J. Laskin, A. Laskin and S. A. Nizkorodov, Formation of nitrogen- and sulfur-containing light-absorbing compounds accelerated by evaporation of water from secondary organic aerosols: brown carbon from droplet evaporation, *J. Geophys. Res. Atmospheres*, 2012, **117**, 1–14.

81 *Toxic substances control act*, U.S. Environmental Protection Agency, Washington, DC, USA, 1976.

82 Final Report on the Safety Assessment of Benzaldehyde, *Int. J. Toxicol.*, 2006, **25**, 11–27.

83 Final Report on the Safety Assessment of BHT, *Int. J. Toxicol.*, 2002, **21**, 19–94.